Astron. Astrophys. 358, 639–650 (2000)

ASTRONOMY AND ASTROPHYSICS

The atmospheric parameters and chemical composition of early B-type giants in h and χ Persei

M. Vrancken[1], **D.J. Lennon**[2], **P.L. Dufton**[3], **and D.L. Lambert**[4]

[1] Royal Observatory of Belgium, Ringlaan 3, 1180 Brussel, Belgium
[2] Universitätssternwarte München, Scheinerstrasse 1, 81679 München, Germany
[3] The Department of Pure and Applied Physics, The Queen's University of Belfast, Belfast BT7 1NN, Ireland
[4] Department of Astronomy, University of Texas, Austin, TX 78712, USA

Received 23 September 1999 / Accepted 7 April 2000

Abstract. Atmospheric parameters and surface chemical compositions are presented for eight stars, classified as B1 or B2 but with a range of luminosity classes, in the northern double cluster h and χ Persei. Echelle spectroscopy (covering the wavelength region 3900 to 4700 Å) and grating spectroscopy (of the Balmer, Hγ and Hβ lines) were analysed using non-LTE synthetic spectra based on LTE line-blanketed atmosphere structures. High microturbulences are found in our sample, and this quantity must be included in the computation of the non-LTE level populations; its effect is generally to decrease the derived metal abundances by typically 0.1 dex but by up to 0.4 dex. Our absolute abundances are in reasonable agreement with those previously found for main sequence B-type stars, while we find some evidence for small abundance variations (particularly for nitrogen) within our sample. One star (BD+56 678) appears to be a spectrum variable and at two epochs shows a highly enriched nitrogen spectrum. Our atmospheric parameters imply that two stars have previously been mis-identified as main sequence objects and a distance modulus, at the higher end of the values previously deduced. The observational HR diagram is consistent with stellar evolutionary models that explicitly include the effects of rotation.

Key words: line: formation – stars: abundances – stars: early-type – stars: evolution – Galaxy: open clusters and associations: individual: h and χ Persei

1. Introduction

The structure and chemical composition of B-type stellar atmospheres have received considerable attention in recent years (see, for example, the recent Boulder-Munich workshop - Howarth, 1998). Main-sequence stars have been used widely to investigate the chemical homogeneity of our own Galaxy (see, for example, Gies & Lambert 1992, Smartt et al. 1996b, Smartt & Rolleston (1997) and the Magellanic Clouds (see, for example, Rolleston et al. 1993, 1996, 1999). Supergiants can provide information on more distant galaxies (e.g. M31: McCarthy et al. 1995; M33: Monteverde et al. 1997 and the preliminary results for NGC 2403 reported in Kudritzki 1998). Although B-type stars in the solar neighborhood imply a below solar oxygen abundance (Gies & Lambert 1992, Kilian 1992), their agreement with Orion H II region results has been interpreted as implying that B-type star results may be more representative of the local (gas plus dust) ISM (Savage & Sembach 1996) than the Sun. Indeed, main sequence B-type stars in the Orion association have also been used to search for an enhanced oxygen signature of Type II supernova ejecta in its youngest subgroups. (Cunha & Lambert 1992; 1994).

However, there are other possible evolutionary processes which may be relevant to the interpretation of B-type star abundances. Lyubimkov (1991) claimed that the nitrogen abundance increases significantly with evolutionary age. Gies & Lambert (1992) subsequently suggested that this conclusion could have resulted from the assumption of a fixed microturbulent velocity for all stars regardless of their evolutionary status, although Lyubimkov (1996) disputes this interpretation. Gies & Lambert (1992) do suggest however that some stars in their sample show evidence for moderate carbon and nitrogen anomalies consistent with some contamination by CN-cycled material. In addition, B-type stars used in Galactic abundance gradient studies also appear to display an anomalously large scatter in their nitrogen abundances compared to that of oxygen (Smartt et al. 1996a), while Lennon et al. (1996) have discovered two main sequence B-type stars in the Small Magellanic Cloud with significantly enhanced nitrogen. Furthermore, a non-LTE model atmosphere analysis by McErlean et al. (1999) has identified a group of chemically processed supergiants from a spectroscopic survey of bright Galactic supergiants (Lennon et al. 1992). It has been suggested that these nitrogen enrichments are the result of mixing processes operating during the main sequence stage, an idea originally suggested by Walborn (1976) to explain the OBN stars, and first investigated theoretically by Paczynski (1973). Rotationally induced mixing is currently the favoured mechanism and has been discussed by Maeder (1987), Langer (1992) and Denissenkov (1994), with more recent predictions concerning the effects on surface abundances being produced by Fliegner et al. (1996) and Talon et al. (1997).

Send offprint requests to: Philip Dufton (P.Dufton@qub.ac.uk)

We therefore decided to observe a sample of B-type stars within the same cluster at different evolutionary stages, but lying within a narrow effective temperature range. This should minimize possible differential systematic effects which may be present between hot and cool stars (see Kilian 1992, 1994). Our objectives were:

- To investigate the reliability of non-LTE model atmosphere techniques for stars evolving away from the zero age main sequence, and in particular the role of microturbulence.
- To search for signatures of CN-cycled material in more evolved B-type stars and in the Be-type stars.
- To compare the atmospheric parameters of the more evolved stars with the predictions of stellar evolution calculations that include the effects of rotation.

The double cluster h and χ Persei (NGC 869 and NGC 884), is an ideal candidate, being one of the richest concentrations of early-type stars in the northern hemisphere (Oosterhoff 1935). It has an age of just over 10 million years, a main sequence turn-off around spectral type B1/B2, and includes many early-B-type giants and supergiants.

The target selection, observations and reduction procedures are discussed in Sect. 2. The model atmosphere calculations, together with the methods used to estimate atmospheric parameters and chemical compositions are presented in Sect. 3, which are then discussed in Sect. 4.

2. Observations and reduction

Targets were initially chosen on the basis that they are members of the h and χ Persei double cluster (Johnson & Morgan 1955; Wildey 1964) and had spectral types between B1 and B3; additionally preference was given to targets that had evolved away from the main sequence. These criteria allowed a nearly complete sampling of the evolved population over the relevant range of spectral types, and also with sufficient coverage of targets whose spectral type implies that they are near to the hydrogen burning main sequence. Spectral types, magnitudes and Strömgren photometry for the targets are listed in Table 1 and are taken from Schild (1965), Slettebak (1968), Crawford et al. (1970) and Tapia et al. (1984). Spectroscopy was undertaken at the McDonald Observatory of the University of Texas from the 22 to 28 November 1995, inclusive. The first three nights were devoted to obtaining profiles for the broad hydrogen lines using a grating spectrograph, while during the latter four nights, the targets were re-observed using a crossed echelle spectrograph principally to measure the metal line spectra. These two sets of observations are discussed separately below.

2.1. Grating spectroscopy

Spectra were obtained using grating C (operating in the second order) at the coudé focus of the 2.7m telescope. The detector was a Tek CCD, which was binned by a factor of two in the direction normal to the dispersion direction. The spectral coverage was approximately 220 Å with a pixel size of 0.4 Å and a spectral resolution of 0.8 Å (full-width-half maximum). Two wavelength regions were considered centred on Hγ and Hβ and total exposure times (normally broken into two separate exposures) were chosen to achieve signal-to-noise ratios per wavelength channel normally in excess of 200. All targets were observed in the Hγ region though the observing time available was only sufficient for a partial coverage of our sample in the Hβ region. Details of the regions observed and the estimated signal-to-noise ratios are listed in Table 1. The latter were estimated from least-squares polynomial fitting of regions that were believed not to contain absorption lines. As such they are likely to be underestimates but provide an insight into the quality of the spectra.

The images were reduced using IRAF and standard procedures (see for example Gies & Lambert 1992). Wavelength-calibrated spectra were then transferred to the Starlink package DIPSO (Howarth et al. 1995) for subsequent analysis.

2.2. Echelle spectroscopy

Spectroscopy was undertaken using the Sandiford Cassegrain echelle spectrograph (McCarthy et al. 1993) and an EG&G Reticon CCD at three different grating positions centred at wavelengths 4050, 4460, and 4180 Å. Each setting provided complete wavelength coverage (i.e. the echelle orders overlapped) of 300–400 Å, with a spectral resolution of better than 0.2 Å. The choice of the first two settings was made primarily to ensure nearly complete wavelength coverage from 3900 to 4700 Å; the third position was chosen so as to improve the signal-to-noise ratio in the overlap regions with the other settings. The wavelength positions were fine tuned to ensure that contamination from the zero order beam did not affect any important spectral features. The wavelength regions observed are again listed in Table 1 together with estimates of the signal-to-noise ratio deduced as discussed below.

The images were reduced to multiple single-order spectra using the IRAF echelle package; the procedures adopted were similar to those discussed by Lennon et al. (1996). The spectra were then transferred to the Starlink DIPSO package for further manipulation. For all spectra, the widths of the lines were far larger than the instrumental profile full-width-half-maximum (FWHM) and are probably dominated by Doppler broadening due to stellar rotational or atmospheric velocity fields. In Table 1, we list typical values for the FWHM deduced by fitting Gaussian profiles to some relatively strong metal lines (e.g. the O II multiplet near 4070 Å and the Si III multiplet near 4560 Å). Normalization for each order was then achieved by fitting low-order polynomials to spectral regions that we believed not to contain absorption lines. These individual orders were then merged together for any given grating setting to provide a single normalized spectrum; the validity of this procedure for lines in overlapping orders was checked manually. The signal-to-noise ratio was then estimated from continuum regions in the merged spectra. Note that these ratios should only be considered as indicative as they will vary both across and between individual orders owing to variations in the spectrograph sensitivity.

Table 1. Observational details of the program stars. The identifications in the second column are from Oosterhoff (1935). Note that in the present analysis we find that the luminosity class of BD +56 502 and BD +56 510 is III rather than V. Columns 8–12 inclusive give the S/N ratios of the observed spectra. The FWHM line widths listed in the last column are derived from fitting Gaussian profiles to the strong O II multiplet near 4070 Å and the Si III multiplet near 4560 Å.

Star		Sp. Type	V	(b−y)	m_1	c_1	coudé		Cassegrain			FWHM
							Hγ	Hβ	4020 Å	4550 Å	4200 Å	Å
HD 14052	NGC 869−662	B1 Ib	8.18	0.259	−0.070	0.087	210	320	140	190	110	1.1
HD 14053	NGC 869−612	B2 II	8.41	0.255	−0.051	0.070	400	190	80	140	100	0.8
HD 14443	NGC 884-2227	B2 Ibp	8.05	0.328	−0.084	0.111	370	230	150	200	130	0.9
BD +56 502	NGC 869-717	B1 V	9.28	0.272	−0.039	0.106	250	210	120	150	80	1.5
BD +56 510	NGC 869-843	B1.5 V	9.32	0.277	−0.050	0.166	250	200	110	130	110	1.9
BD +56 511	NGC 869-847	B3 III	9.11	0.345	−0.087	0.143	300	190	100	130	80	1.5
BD +56 576	NGC 884-2311	B2 III	9.39	0.282	−0.064	0.160	270	-	120	100	110	0.4
BD +56 578	NGC 884-2371	B2 IIIe	9.25	0.307	−0.078	0.129	300	250	170	150	90	1.5

Equivalent widths were deduced from the merged normalized spectra by fitting multiple Gaussian profiles to selected wavelength regions using non-linear least squares optimization procedures. Tests indicated that the line strength estimates were not particularly sensitive to the choice of profile shape. Where possible, exposures with different grating settings were combined (after checking for possible wavelength shifts). A low-order polynomial was also included in the fitting procedure to allow for inadequacies in the original normalization. Further details on the fitting procedures can be found in Smartt et al. (1996a). The equivalent widths of approximately 90 individual lines or blends are too extensive to be listed here but are available from either from the VizieR Catalogue service at the CDS or from the authors.

The least squares optimization yielded formal error estimates but we have instead adopted a more qualitative approach as follows – (a) formal errors normally less than 5%; the line is well observed and normalization of the continuum is convincing, (b) formal errors normally less than 10%; the line is clearly present and there are no significant normalization difficulties, (c) either weak lines or stronger lines with blending or normalization problems. The line strength measurements should be treated with some caution, (d) lines identified during the optimization procedure by coincidence with the appropriate laboratory wavelengths (after correction for the stellar radial velocity). However the fits were sometimes unconvincing and the line strength measurements may be unreliable.

We note that the formal errors should be treated with caution and believe that they underestimate the uncertainties. In general, we would expect the *class a* measurement to be accurate to typically 10%, whilst those of *class b* should be reliable to 20%.

3. Model atmosphere analysis

3.1. Model calculations

Model atmospheres were taken from the LTE line blanketed grid of Kurucz (1992) for solar abundances and the line-formation problem was solved using the programmes DETAIL and SURFACE (Butler & Giddings 1985). The problem was tackled in two stages; term populations were computed with DETAIL, while fine-structure populations and emerging fluxes were computed with SURFACE. The following model atoms were adopted: H (Herrero 1987); He (Husfeld 1986); C II (Eber & Butler 1988); N II (Becker & Butler 1989); O II (Becker & Butler 1988); Mg II (Mihalas 1972; Butler, priv. comm.); Al III (Dufton et al. 1986); Si II–III–IV (Becker & Butler 1990).

The grids of line profiles presented in Vrancken et al. (1996) had to be extended towards higher microturbulences and lower gravities, as summarized below. For the silicon spectrum:

- $T_{\rm eff}$: 19 000 to 25 000 in steps of 1000 K
- $\log g$: 3.0 to 3.8 in steps of 0.2 dex
- $\log \epsilon$(Si): −5.4 to −4.4 in steps of 0.2 dex
- $v_{\rm turb}$: 9.0 to 21.0 km s^{-1} in steps of 3.0 km s^{-1}.

For the other elements:

- $T_{\rm eff}$: 20 000 – 22 000 – 24 000 K
- $\log g$: 3.0 – 3.5 – 4.0 dex
- Abundances from -1.0 dex to +0.5 dex relative to the solar value, in steps of 0.5 dex
- $v_{\rm turb}$: 5 to 20 km s^{-1} in steps of 5 km s^{-1}.

One important difference with earlier work is that the level populations were computed with the effect of microturbulence included in DETAIL (the 'non-classical effect' of microturbulence) and not simply in the emergent line profiles; a similar approach has been advocated for supergiant stars by McErlean et al. (1998, 1999). Including microturbulence in this non-classical way generally increased calculated line strengths and we investigated its importance as follows. Synthetic spectra were computed including microturbulence only in the SURFACE runs to simulate 'observed' spectra. These were then re-analysed using the non-classical approach to microturbulence. The principal conclusions of such tests, based on the lines used for the abundance analysis of BD +56 576 can be summarized as follows:

- Carbon: Lines of C II showed the largest effects; for example, the mean abundance was reduced by 0.2 dex even for a moderate microturbulence of $v_{\rm turb}$=10 km s^{-1} and by up to 0.45 dex for the doublet at 4267 Å.

Table 2. Atmospheric parameters derived from the hydrogen and silicon lines are given in Columns 2 and 3. In the fourth column values of $v \sin i$ are given; (1) indicates the values from Slettebak (1968) and (2) those from Slettebak (1985).

Star	$T_{\rm eff}$ K	$\log g$ dex	$v \sin i$ km s^{-1}
HD 14 052	21 500±500	3.00±0.05	$<50^{(1)}$
HD 14 053	22 500±500	3.20±0.05	–
HD 14 443	21 500±500	3.00±0.05	$<50^{(1)}$
BD +56 502	23 000±1500	3.40±0.10	$60^{(1)}$
BD +56 510	21 500±1500	3.40±0.10	–
BD +56 511	21 000±500	3.10±0.10	$100^{(2)}$
BD +56 576	22 500±500	3.40±0.05	$<50^{(1)}$
BD +56 578	22 500±500	3.20±0.05	$100^{(2)}$

– Nitrogen & Oxygen: The abundances changes were relatively small for these elements corresponding to ≃0.1 dex for a $v_{\rm turb}$=15 km s^{-1} but increasing with line strength, to approximately 0.15 dex. This in turn will lead to slightly smaller estimates for the microturbulence.
– Aluminum: The effects for Al III lines were negligible.
– Magnesium: This abundance was deduced from one relative strong Mg II line at 4481 Å where the change was typically 0.1–0.2 dex for a $v_{\rm turb}$=15 km s^{-1}.
– Silicon: All three ionization stages of silicon were affected and hence the estimates of effective temperature were not significantly changed. For a $v_{\rm turb}$=15 km s^{-1}, the abundance estimates were typically decreased by 0.1–0.2 dex.

3.2. Determination of the atmospheric parameters

Our procedures for estimating atmospheric parameters followed standard methods as discussed in Vrancken et al. (1997) and used previously in other studies (see, for example, Becker & Butler 1990 and McErlean et al. 1999). Hence only a brief summary will be given here, with further details being available in the above papers.

Effective temperatures and logarithmic gravities were derived from the silicon ionization equilibrium (Si II λ4128.1, λ4130.9, the Si III $\lambda\lambda$4552.6, 4567.8, 4574.8 triplet and Si IV λ4116.1 – λ4088.6 and λ4631.2 were blended and not considered) and from the Hγ and Hβ line profiles. Since the strength of the silicon lines also depends on the adopted abundance and the microturbulence, the four parameters were determined simultaneously. The adopted $v_{\rm turb}$ was the value for which the silicon lines from different ionization stages were most consistent with the scatter in the estimated abundances being minimized. Other species can also be considered, for example the O II spectrum in early B-type stars is one of the richest. Values of $v_{\rm turb}$ derived from the O II lines were in general larger than those obtained from the silicon lines and as discussed by Vrancken et al. (1997), errors in oscillator strengths may be a contributing factor. These can be eliminated by using lines belonging to one multiplet, and multiplet 1 at approximately 4650 Å is well suited for this purpose since its lines cover a large range of equivalent widths. Indeed the $v_{\rm turb}$ estimates derived from this multiplet were lower than those derived from all O II lines but still larger than the Si III values. However a complicating factor is that the weaker O II lines were difficult to measure for stars with large projected rotational velocities, while the stronger lines were often badly blended. As there was no obvious reason to prefer any one criterion, the $v_{\rm turb}$ estimates derived from the silicon lines have been adopted.

The physical mechanism for the large microturbulent velocities in giant and supergiant stars has been extensively discussed (see, for example McErlean et al. 1998, 1999 and references therein) and its origin is unclear. The direct comparison of the observed and theoretical profiles to search for additional broadening would be very attractive as this would provide direct evidence for whether the microturbulence was really a velocity field or simply an artifact of the simplifications made in our analysis. In fact we have used this approach successfully for two very narrow line stars, PG 0832+676 (Hambly et al. 1996) and HD 83206 (Lehner et al. 2000). Both these stars have effectively zero projected rotational velocity and relatively high gravities (log g≃4.2) and are probably evolved post-HB stars. Even in these cases, it is difficult to distinguish between rotation, $v_{\rm rot}$ and microturbulence; for example, for HD 83206 the profiles for $v_{\rm turb}$=0 & $v_{\rm rot}$= 5 km s^{-1} and $v_{\rm turb}$=3 & $v_{\rm rot}$= 0 km s^{-1} are virtually identical for a given equivalent width. Unfortunately all our targets have line widths that are significantly large than the intrinsic profiles i.e. all our stars have significant rotational broadening. Numerical tests show that in such cases it is impossible to distinquish between the rotationally broadened profiles for calculations using different microturbulence.

Metal abundances (summarized in Table 3) were determined by interpolation in the grids of equivalent widths discussed in Sect. 3.1. Equivalent widths classified as quality *d* were not considered. Abundances corresponding to the higher $v_{\rm turb}$ derived from the O II lines are also given and are identified in Table 3 and in the text by being enclosed in round brackets. The abundances derived from the peculiar spectrum of BD +56 578 will be discussed separately.

The errors in the final abundances induced by changes of ±1000 K in $T_{\rm eff}$ and ±0.2 dex in $\log g$ are of the order of 0.05–0.10 dex. A comparison of the abundances for the two sets of microturbulence estimates, shows that nitrogen and aluminum were relatively insensitive to this parameter with other elements showing changes of up to 0.3 dex.

4. Results and discussion

4.1. Atmospheric parameters and spectral types

The stars can be divided into two groups; five fainter stars (identified by their BD number) previously classified as giants or dwarfs, and the 3 brighter giants and Ib supergiants (identified by their HD number).

Table 3. Microturbulent velocities and abundances by number relative to the total number density. Two microturbulences are given and are derived from the silicon lines or from an analysis of the O II-multiplet 1 (in round brackets). The number of lines used for each abundance estimate is listed in square brackets. Errors are the 1σ deviations of abundances from single lines. Abundances within round brackets are those computed for the $v_{\rm turb}$ derived from the oxygen lines. The C, N and O abundances of BD +56 578 are discussed in Sect. 4.3.1.

Star	$v_{\rm turb}$	$\log\epsilon$(C)	$\log\epsilon$(N)	$\log\epsilon$(O)	$\log\epsilon$(Mg)	$\log\epsilon$(Al)	$\log\epsilon$(Si)
HD 14 052	12	-4.24 ± 0.22 [3]	-4.65 ± 0.24 [13]	-3.32 ± 0.33 [24]	-5.05 [1]	-6.23 ± 0.04 [2]	-4.85 ± 0.05 [4]
	(21)	(-4.33)	(-4.70)	(-3.55)	(-5.20)	(-6.33)	(-5.13)
HD 14 053	9	-4.00 ± 0.17 [2]	-4.49 ± 0.23 [13]	-3.08 ± 0.33 [25]	-4.88 [1]	-5.99 ± 0.05 [2]	-4.73 ± 0.28 [4]
	(18)	(-4.33)	(-4.58)	(-3.44)	(-5.03)	(-6.15)	(-5.00)
HD 14 443	12	-4.06 ± 0.21 [3]	-4.76 ± 0.20 [12]	-3.50 ± 0.26 [22]	-4.80 [1]	-6.04 ± 0.06 [2]	-4.87 ± 0.26 [6]
	(21)	(-4.21)	(-4.80)	(-3.70)	(-5.01)	(-6.16)	(-5.10)
BD +56 502	9:	-4.19 ± 0.11 [2]	-4.58 ± 0.18 [8]	-3.24 ± 0.11 [18]	–	-6.24 ± 0.02 [2]	-4.87 ± 0.11 [4]
	(13:)	(-4.34)	(-4.64)	(-3.42)	–	(-6.27)	(-5.06)
BD +56 510	9:	-4.29 ± 0.19 [2]	-4.47 ± 0.29 [6]	-3.40 ± 0.15 [13]	–	-6.29 [1]	-5.12 ± 0.15 [4]
	(13:)	(-4.43)	(-4.44)	(-3.54)	–	(-6.33)	(-5.22)
BD +56 511	9	-4.40 ± 0.20 [2]	-4.74 ± 0.11 [2]	-3.27 ± 0.24 [17]	–	–	-4.70 ± 0.10 [4]
	(13:)	(-4.54)	(-4.83)	(-3.44)	–	–	(-4.93)
BD +56 576	9	-4.11 ± 0.18 [3]	-4.65 ± 0.22 [14]	-3.43 ± 0.14 [23]	-4.92 [1]	-6.03 ± 0.02 [2]	-4.91 ± 0.10 [4]
	(13)	(-4.22)	(-4.69)	(-3.59)	(-5.01)	(-6.06)	(-5.02)
BD +56 578	9	(*)	(*)	(*)	-4.90 [1]	-6.01 ± 0.03 [2]	-5.18 ± 0.13 [4]
	(13:)				(-4.99)	(-6.05)	(-5.42)

4.1.1. The giants and dwarfs

Altough these stars have luminosities classes ranging from III to V, their gravities only cover a small range. Indeed all appear to be evolved and in particular BD +56 502 and BD +56 510 have surface gravities of $\log g$=3.4 which are comparable to those of the luminosity class III stars. Moreover their visual magnitudes are also similar to those of the giants in our sample. Hence their previous spectral classification as luminosity class V objects appears to be erroneous. Since they have relatively high projected rotational velocities, we suspect that this may have contributed to the mis-classification. Additionally the estimated effective temperature for BD +56 511 is higher than expected for a B3 star, again indicating the limitations of spectral types even for these reasonably bright stars.

Below we briefly discuss each star in turn:

BD +56 576: With the sharpest lines amongst our sample (see Table 1), all three ionization stages of silicon were observed leading to a secure effective temperature estimate. No Balmer line emission has been reported for this star, while Krzesinski & Pigulski (1997) sugests it is an eclipsing binary (with a period of 102.1 days or a sub multiple thereof), which is consistent with the different radial velocities found by Liu et al. (1991) and Dufton et al. (1990). The latter authors suggest that it is a single lined spectroscopic binary and indeed there is no evidence for a secondary in our spectra.

BD +56 502: Torrejón et al. (1997) have reported emission peaks in both the Hα and Hβ lines, while Waelkens et al. (1990) observed variations in its colors and visual magnitude, which they interpreted as evidence of possible emission-line behaviour. This object is probably a weak Be-type star which we have observed in quiescence,

BD +56 510: No evidence is found for Be-type behaviour

BD +56 511: There is evidence of emission in Hβ, the line profile showing some infilling with a double-peaked profile. Weak emission in Hα was previously reported by Merrill & Burwell (1950) and Bidelman (1965), while Slettebak (1985) observed Hα to be in emission and Hβ in absorption. Owing to this infilling by emission, only Hγ could be used for the gravity determination.

BD +56 578: This star displays emission on the red side of Hβ, while Hγ is also slightly asymmetric. Emission was found by Schild (1965), while Slettebak (1985) reported Hβ to be weak but still in absorption and Hα to be filled in by emission up to the continuum level. More recent spectra of the first three Balmer lines of this star (Torrejón et al. 1997) also show that the red wing of all three lines is slightly filled in by emission. Krzesinski & Pigulski (1997) have suggested that this star could be a binary (and give a tentative period of about 2.6 days), a suggestion supported by the range of reported radial velocities (Liu et al. 1991).

We also find evidence for significant velocity shifts. For example, the radial velocity of the three sets of echelle spectra taken on consecutive nights (26 to 28 November) are -33 ± 14 (sample standard deviation) from 14 measurements, $-30\pm14\,{\rm km\,s^{-1}}$ from 13 measurements and $-161\pm7\,{\rm km\,s^{-1}}$ from 10 measurements. The wavelength coverage, emission in the hydrogen lines and lack of strong metal lines in the Coudé spectra make them less suitable for determining reliable radial velocities. However for the Hγ and Hβ regions observed on the 22 and 24 November, we obtain radial velocities estimates from the hydrogen and helium lines of $\simeq -105\,{\rm km\,s^{-1}}$ and $\simeq -175\,{\rm km\,s^{-1}}$ respectively. Moreover if radial velocity variations did exist, they might also explain the asymmetric Balmer line profiles seen here and by Torrejón et al. (1997).

Table 4. The mean abundances derived in the present study, compared with abundances of early B-type stars from the literature.

Object(s)	$\log\epsilon$(C)	$\log\epsilon$(N)	$\log\epsilon$(O)	$\log\epsilon$(Mg)	$\log\epsilon$(Al)	$\log\epsilon$(Si)	$\log(\frac{\epsilon}{\epsilon_\odot})$
This study[1]	-4.18	-4.62	-3.32	-4.91	-6.14	-4.86	-0.49 ± 0.19
	±0.14	±0.11	±0.14	±0.10	±0.13	±0.14	
Kilian[2]	-3.78	-4.22	-3.48	-4.62	-5.88	-4.84	-0.30 ± 0.10
Kilian (cool)[3]	-3.77	-4.41	-3.56	-4.68	-6.19	-5.19	-0.45 ± 0.18
G&L[4]	-3.84	-4.23	-3.36	–	-5.59	-4.46	-0.17 ± 0.17
#201[5]	-3.80	-4.42	-3.41	-4.62	-5.85	-4.72	-0.29 ± 0.09
Sun[6]	-3.48	-3.99	-3.11	-4.46	-5.57	-4.49	

[1] Mean of the abundances derived for the present sample; BD +56 578 is not included
[2] Mean of sample of 21 early B-type stars studied by Kilian (1992, 1994)
[3] Mean of the 4 coolest stars in the sample considered in [2]
[4] Gies & Lambert (1992)
[5] NGC 2244-201 (Vrancken et al. 1997)
[6] Anders & Grevesse (1989)

The CNO linestrengths in the echelle spectra of BD +56 578, for the three different wavelength ranges, are inconsistent as discussed in Sect. 4.3.1. In determining the stellar parameters, we have assumed that the Si IV and Si III lines observed in the two spectral regions can be combined (i.e. the silicon spectra is not variable). Additionally, the Hβ line was not considered, and as the core of Hγ may also be affected by emission, its width at an intensity level of about 0.9 was used for the gravity determination.

4.1.2. The bright giants/supergiants

HD 14052 (B1 Ib) and HD 14443 (B2 Ibp) have very similar Hγ and Hβ profiles, but these lines are clearly somewhat deeper and broader in HD 14053 (B1 II). In all cases, their atmospheric parameters are consistent with their spectral types. HD 14053 is a β Cepheid variable (Hill 1967), while none of the stars shows any evidence for emission in their Balmer lines.

4.2. Absolute Metal abundances

We first compare our abundances with those found from other analyses of B-type stars. These have concentrated on dwarfs and subgiants - indeed this was one of the motivations for the present study. 'Standard' B-type star abundances are defined here as those derived using techniques similar to our methods, namely LTE line blanketed model atmospheres and NLTE line formation calculations. Note that these will not necessarily be the most reliable results but will form a suitable basis for comparison. Kilian (1992, 1994), Gies & Lambert (1992; see also Cunha & Lambert 1992, 1994) and Vrancken et al. (1997) all used such technigues. However one important difference is that they treated microturbulence in the standard way.

Kilian (1992, 1994), adopted the atmospheres of Gold (1984), which include less line blanketing than those of Kurucz (1992). The most important consequence will be a different temperature scale (see Cunha & Lambert 1994). Kilian however used identical atomic data and model atoms as here and similar techniques to derive the atmospheric parameters and abundances. Gies & Lambert (1992) on the other hand used Kururcz models but deduced atmospheric parameters from photometric calibrations and hydrogen line profiles, although additional temperature corrections, based on the Code et al. (1976) temperature scale, were applied. Abundances were obtained from interpolation in the same non-LTE grids as were used by Kilian with corrections being applied to allow for trends in abundance with temperature and to account for differences in atomic data. Vrancken et al. (1997) used similar methods to those used here but unfortunately considered only a single star, NGC 2244-201, with a relatively large temperature ($T_{\rm eff}$=27 300 K).

In Table 4 our mean absolute abundances are compared with those of these previous investigations. Also listed is the mean unweighted differences between the hot stars abundances and the sun ($\log(\frac{\epsilon}{\epsilon_\odot})$). In addition, since Kilian noted a trend of abundance with effective temperature in her results, we also list results for the four coolest stars in her sample. Below we discuss the individual elements in turn.

4.2.1. Carbon

The carbon abundance includes estimates from the 4267 Å doublet which is well known to be a problematic line for absolute carbon abundances in B-type stars (Lennon 1988). Neither Kilian nor Gies & Lambert considered this transition but Vrancken found a mean carbon abundance of 8.08 dex for the two lines upon which most of the present results are based, 4267 and 4075 Å. A recent non-LTE investigation of the line formation problem for the 4267 Å line by Sigut (1996) shows that the model atom of Eber & Butler (1988) needs to be extended, while our more consistent treatment of the microturbulence will have reduced the mean carbon abundance by 0.2 to 0.4 dex. We conclude that while there are systematic differences in the abundances found here and in previous work, these are probably due to differences in the features observed and in the model atmosphere techniques.

4.2.2. Nitrogen

Our mean nitrogen abundance is approximately 0.4 dex below that of Kilian and Gies & Lambert, but only 0.2 dex below Vrancken's result for NGC 2244-201. We also note that the cool stellar subset of Kilian has an abundance only 0.2 dex higher, and the different treatment of microturbulence would reduce this discrepancy by approximately 0.1 dex.

4.2.3. Oxygen

Our mean oxygen abundance derived is larger by 0.24 dex than that of the Kilian cool stellar subset but agrees well with the mean values for the complete Kilian sample, with Gies & Lambert and with Vrancken. For the elements studied here, oxygen both yields the most internally consistent estimates, and also agrees best with the results from other studies of less evolved B-type stars.

4.2.4. Magnesium

The magnesium abundance is derived from the 4481 Å doublet and our treatment of the microturbulence will lead to a decrease of approximately 0.1 dex. Since our mean abundance is only 0.2 dex lower than the Kilian cool sample mean, we believe that our results are consistent with those for main sequence objects.

4.2.5. Aluminium

For the Aluminium abundances listed in Table 4, there are significant differences between the Kilian (and Vrancken) and Gies & Lambert results (approximately 0.3 dex). The Kilian cool sample gives a mean abundance in excellent agreement with our result (the different treatments of the microturbulence have a negligible effect).

4.2.6. Silicon

Silicon is a key element as it is used in the determination of the effective temperatures. Allowing for the different treatments of the microturbulence, our results agree well with Kilian and Vrancken although they are still low compared to Gies & Lambert. However the mean silicon abundance for the Kilian cool stellar sample abundance is almost 0.5 dex lower and we have no explanation for this discrepancy.

4.2.7. General

The discrepancies between the mean abundances derived here and those reported in the literature can be partially traced to the different treatment of the microturbulence, although the use of different model atmospheres, temperature scales, atomic data and samples of lines may also be significant contributing factors. Nevertheless, the results, particularly for nitrogen, oxygen, magnesium and silicon are encouraging and imply that plane parallel non-LTE model atmosphere techniques may be adequate for B-type giants. This will be particularly important for investigations of other galaxies, where observations will necessarily be limited to the more luminous B-type stars. Furthermore, the abundance estiamtes from different stars show reasonable internally consistency as is indicated by the relative small standard deviations.

It is interesting to note that all the analyses of B-type stars listed in Table 4 lead to lower metallicities than the sun. The differences range from –0.17 dex (which may not be significantly significant) for Gies & Lambert (1992) to –0.49 dex in the current study. As noted above, our inclusion of the microturbulent velocity into the statistical equilibrium calculations leads to abundance estimates that are typically 0.1 to 0.2 dex lower than those in previous non-LTE calculations. When this is taken into account, the metallicity deduced for the h and χ Persei targets relative to the sun lies in the middle of the range found by Gies & Lambert and Kilian. However, it is unclear whether the differences in metallicities found for the hot star samples and the sun is real.

In the next section we consider whether there is any evidence for abundance variations *within* our sample.

4.3. Relative abundances

For all stars (apart from BD +56 578 discussed separately below) the mean CNO abundance ratios were $\log\epsilon$(C)-$\log\epsilon$(N) = +0.44 (0.33) and $\log\epsilon$(O)-$\log\epsilon$(N) = +1.30 (1.14) with a root-mean-square (rms) variation of 0.15 dex. The former agress well with the mean B-type stellar ratio in Table 4, while there is a difference of typically 0.4 dex for latter. However as discussed previously, both our carbon and nitrogen abundances are significantly lower compared to previous work, resulting in high O/N and O/C ratios whereas the C/N ratio remains unchanged.

It is more useful to search for differences between individual objects. We note that although the sum of the CNO abundances should be unaffected by CNO processing, this is dominated by the oxygen abundance and uncertainties therein and hence does not provide a significant constraint. HD 14443 has the highest C/N ratio of the sample, with $\log\epsilon$(C)-$\log\epsilon$(N) = +0.70 (+0.59), despite it being one of the most evolved objects. This star has the lowest nitrogen abundance (although similar to BD +56 511) and was classified as a nitrogen weak star by Walborn (1970). However we emphasis that it is the combination of low nitrogen and high carbon abundance that results in the high C/N ratio. At the other end of the C/N scale, BD +56 510 with $\log\epsilon$(C)-$\log\epsilon$(N)= +0.18 (+0.01), appears to be mildly enhanced in nitrogen and depleted in carbon. This star has the largest value of $v \sin i$ in our sample which implies that there may be a correlation with rotation.

A comparison of N/C ratios and projected rotational velocities listed in Table 2 suggests that there may be a positive correlation. However these rotational velocity estimates are incomplete and we have therefore adopted the full-width-half-maximum line widths listed in Table 1. These will be dominated by rotational (and possibly for the more luminous stars by macroturbulent) velocity broadening and hence will provide

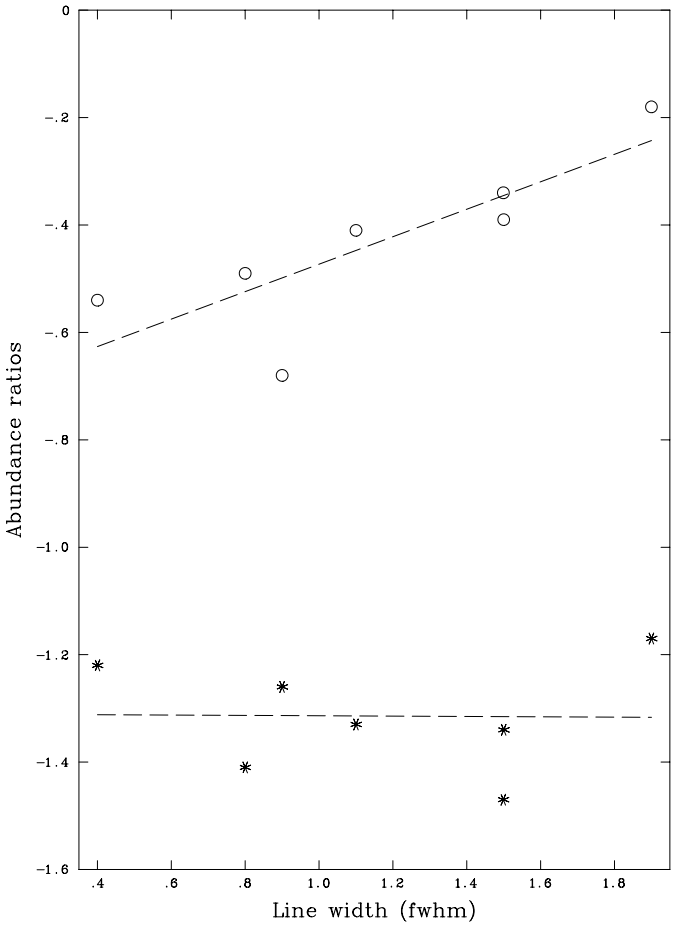

Fig. 1. N/C (circles) and N/O (asterisks) abundance ratios plotted against line widths (in Å). Also shown are linear least square fits.

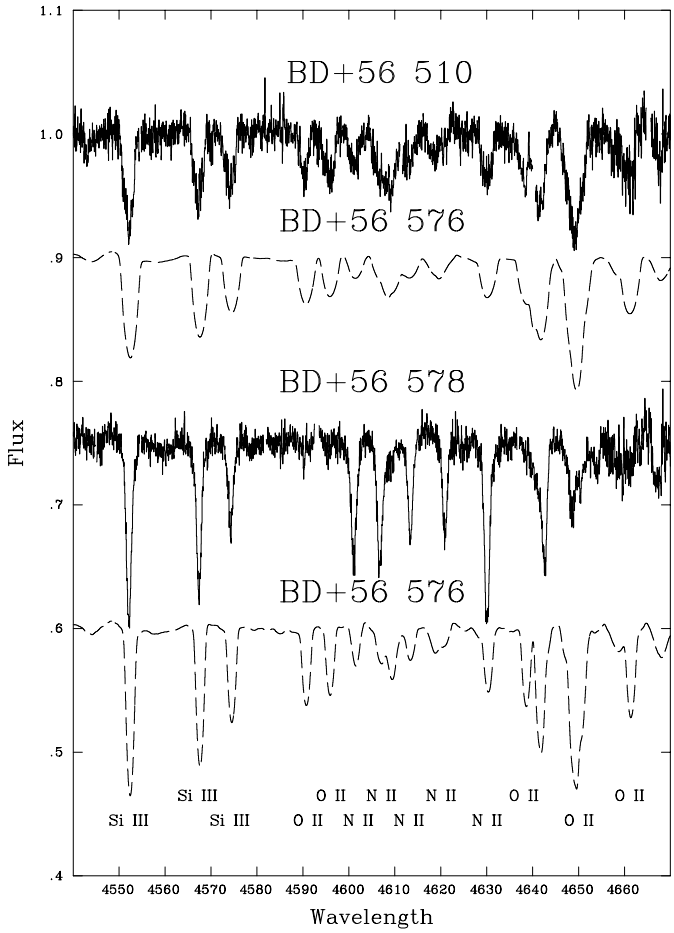

Fig. 2. Upper plots: Comparison of the spectrum of BD +56 510 (histogram) with the rotationally broadened ($v \sin i$=140 km s^{-1}) spectrum of BD +56 576 (smooth line) - the latter has been arbitrarily shifted by 0.1 in the y-axis. Lower plots: Comparison of the spectrum of BD +56 578 with the rotationally broadened ($v \sin i$=80 km s^{-1}) spectrum of BD +56 576 (smooth line). Note that the N II lines are much stronger and O II lines are much weaker in BD +56 578. Both spectra have been shifted along the y-axis to aid comparison.

a consistent estimates of velocity broadening (although these widths will not directly translate into values of $v \sin i$). In Fig. 1, both the N/C and N/O abundance ratios are plotted as a function of these line widths. For the former a significant positive correlation is found, which is consistent with the predictions of stellar evolution calculations including rotation (Denissikov 1994; Talon et al. 1997; Fliegner et al. 1996), where an nitrogen enhancement of a factor of 2–3 together with a smaller carbon deficiency is predicted in the fastest rotators. However the effectively constant N/O abundance ratios appear inconsistent with such a scenario. Hence we conclude that either our observational uncertainties have masked the (smaller) changes predicted for the N/O variations or that our N/C abundance variations are not real but are artefacts of the methods used.

We note that the fast and slow rotators have had abundances estimated from different sets of lines with the former based on fewer and stronger lines (which are more susceptible to microturbulence). Additionally the effect of any abundance changes is relatively modest. This is illustrated in Fig. 2, which compares the spectra of BD +56 510 (which has the broadest metal lines) with that of the slow rotator BD +56 576; the latter has been convoluted with a rotation broadening profile (see Vrancken et al. 1997 for details) with $v \sin i$= 140km s^{-1}, which is appropriate to the spectrum of BD +56 510. Although the nitrogen features in BD +56 510 may be enhanced, the change is modest. A similar comparison was undertaken for the two weak Be-type stars, BD +56 502 and BD +56 511, and again any enhancements of the nitrogen spectra are small.

Hence we conclude that the N/C abundance ratios are consistent with rotational mixing. However given the relatively small magnitude of the abundance changes and the variation in line widths within our sample, these results are by no means conclusive.

4.3.1. BD +56 578

The echelle spectra of BD +56 578, in the three different wavelength ranges, were taken on consecutive nights and show large inconsistencies, especially in the N II and O II lines. Krzesinski & Pigulski (1997), suggest that BD +56 578 is an ellipsoidal

variable/binary with a tentative period of about 2 days and this may be related to these spectral variations.

Another possibility is that two different objects were observed. Support for this is that the observer (PLD) was relatively inexperienced in the use of the 2.1m telescope while observing conditions, with high winds, were difficult. However two pieces of evidence do not support such a mistake. Firstly although the line strengths are peculiar, the line widths measured in the different wavelength regions (reflecting mainly the rotational Doppler broadening) are consistent. For example, the wavelength regions 4065–4080 Å (containing mainly O II lines), 4600–4635 Å (mainly N II lines) and 4220–4245 Å (N II lines) were fitted using the procedures discussed in Sect. 2 and yielded full-width-half maxima of 90.0 ± 2.8, 86.6 ± 1.2 and 87.6 ± 2.4 km s^{-1} respectively. The small differences may reflect additional broadening mechanisms (e.g. instrumental broadening) that do not strictly scale with wavelength but in effect, all the wavelength regions appear to have identical linewidths.

Secondly, the line strengths in the two longer wavelength region are clearly peculiar. As lines of N II and O II have their greatest strength at similar effective temperatures, to first order their line strengths (for a normal composition) have a similar temperature dependence. Hence strong N II coupled with weak O II line strengths are incompatible with a normal composition. To summarize if the observations are of different stars, they have identical line widths, with one of them having an very abnormal composition. Rather we believe that the observations relate to the same star and make this assumption in the following discussion.

The lines in the wavelength region centred at 4020 Å indicate that the carbon, nitrogen and oxygen abundances are very similar to those derived for the normal object BD +56 576. By comparison, the N II lines in the two longer wavelength regions are significantly enhanced and imply an overabundance of approximately 0.6 dex compared to BD +56 576. Several O II lines are not even present in this spectrogram of BD +56 578, while others are at least a factor of two weaker than those in BD +56 576. We also find that C II λ4267 in BD +56 578 is very weak or absent, resulting in an underabundance of at least 1.0 dex. The abundances of magnesium and aluminium, derived from lines in the longest wavelength interval, are normal, while silicon is slightly underabundant (see Table 3). In Fig. 2, the spectrum of BD +56 578 is compared with that of BD +56 576; again the latter has been convolved with a rotational broadening profile ($v \sin i$= 80km s^{-1}) so that the spectra have similar line widths. Note the enhanced N II lines between 4600 and 4630 Å and at 4643 Å in BD +56 578; by contrast the O II lines at 4590, 4596 and 4650 Å are either absent or far weaker than in BD +56 576.

Although the analysis of this peculiar star is very uncertain, the pattern and magnitude of abundance peculiarities are still of interest. The weak carbon, strong nitrogen and, in particular, the weak oxygen line strengths imply the presence of CNO processed material, as opposed to just CN processed material in the second and third nights' observations. It is clear that more observations are essential in order to investigate the nature of this object.

4.4. Distances

Estimates for the distance-modulus to h and χ Per range from 11.17$\pm$0.1(Balona & Shobbrook 1984) to 11.9 (Wildey 1964). Some authors have also claimed that the clusters lie at different distances; Nicolet (1981) finds 11.04$\pm$0.41 and 11.47$\pm$0.42 for h and χ Per respectively while Schild (1967) argued for values of 11.66 and 12.00. To a large extent, these discrepancies can be understood in terms of the stellar samples and the methods used. For example Crawford et al. (1970) obtain a value of 11.4 based upon Stromgren $ubvy$ and Hβ photometry and a calibration of the $M_v - \beta$ relationship. However, their dataset is biased towards the brighter cluster members where evolution effects may have affected their results (Balona & Shobbrook 1984 also use this dataset). Indeed we have already demonstrated that some of the brighter stars, which have been classified as dwarfs, are in fact evolved stars.

Schild (1967) and Wildey (1964) considered fainter main sequence stars and obtain larger distances. Wildey in particular considers main sequence fitting in the range $M_v = -1$ to $M_v = 3$ obtaining a distance modulus of 11.9 with no significant difference between the two clusters (although there is evidence, as discussed by Schild, for a difference in age). We suggest therefore that the smaller distance estimates result from the neglect of evolution in the upper main-sequence.

The distance modulus can be further constrained as B-type stars near to the zero age main sequence (ZAMS) in detached eclipsing binary systems have observed masses in very good agreement with masses derived from evolutionary tracks (see, for example, Schönberner & Harmanec 1995). Two B-type stars in χ Per closer to the ZAMS than the stars considered here have been observed and analysed by Lennon et al. (1988) and Dufton et al. (1990) – Oo2139 and Oo2196, which have logarithmic surface gravities of 4.0 dex and effective temperatures of 21000 K and 20500 K respectively. From the stellar evolution tracks of Heger (1998) we can estimate their masses and luminosities (see Sect. 4.5). Adopting appropriate bolometric corrections, we then obtain absolute visual magnitudes of -2.03 and -1.96 for Oo2139 and Oo2196, which combined with extinction estimates and visual magnitudes give distance moduli of 11.80 and 11.79. These values are in good agreement with Wildey's value of 11.9, the small discrepancy possibly being due to these two stars having evolved further from the ZAMS than those considered by Wildey. We note that a smaller distance modulus of 11.2 would result in masses of only $\sim$4.0 solar masses for these B2V/B1.5V stars. Hence we adopt a value of 11.9 for the distance modulus to both clusters.

4.5. Evolutionary status

Interstellar extinctions were estimated using two separate methods; from a comparison of observed and intrinsic B$-$V colors (as expected from the spectral type), and by a comparison of the

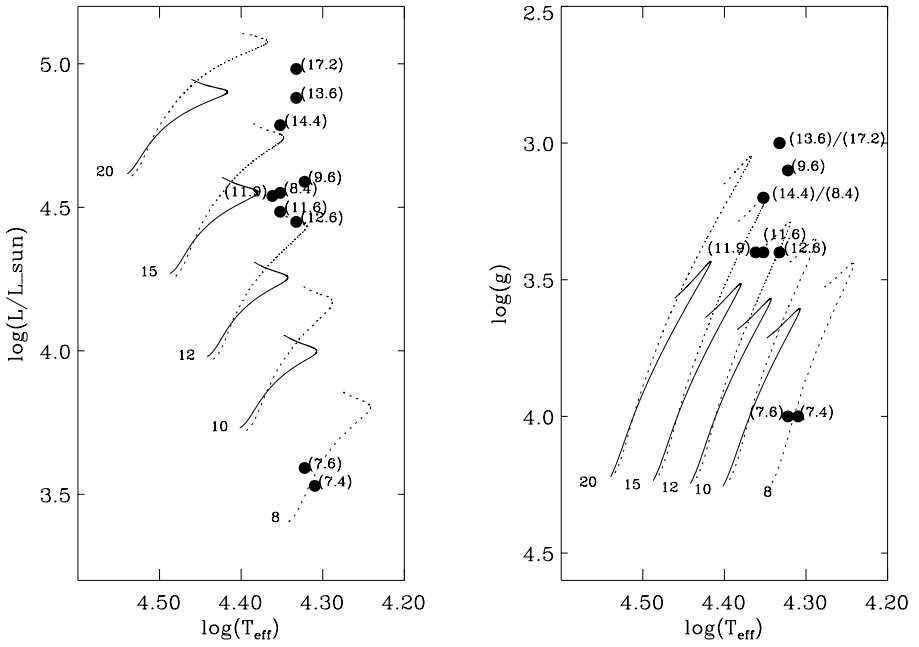

Fig. 3. The positions of the stars of our sample in the $\log T_{\rm eff}$-$\log L/L_{\odot}$ diagram (left) and the $\log T_{\rm eff}$-$\log g$ diagram (right) together with the tracks of Heger (1998) for rotating (dotted lines) and non-rotating (solid lines) stars with Z=0.02. The rotating models are for an initial equatorial velocity of approximately 200km s^{-1}and the tracks are labeled with their stellar masses. The objects are also labeled with their spectroscopically inferred masses (in parentheses) which, by referring to Table 5, may be used to identify each object. Note that some stars in the right-hand panel are co-incident. A distance modulus of 11.9 was adopted for the distance to h and χ Per.

theoretical flux distribution from the atmospheric models with the observed UBV magnitudes. Both methods resulted in very similar values, differing typically by 0.01 in E(B−V) and never more than 0.02 magnitudes. We adopt the results from the flux distribution method, and this technique also provides us with estimates of the the stellar angular radii. Using our adopted distance we can then estimate the radii of our stars, and together with our values of $T_{\rm eff}$ we can estimate the stellar luminosities (designated as 'rad.' in Table 5). Alternatively we can estimate absolute visual magnitudes using our adopted distance modulus and extinction estimates (we assume $R_V = 3.1$), and then use bolometric corrections (implied by the stellar atmosphere flux distributions) to derive bolometric magnitudes and luminosities – designated as 'dist.' in Table 5. Results for the two fainter (near) main sequence stars, Oo2139 and Oo2196 (see Sect. 4.4) are also summarized.

The luminosities deduced from the two methods are similar, although the 'dist' estimates are typically 5–10% higher. Table 5 also lists stellar masses, estimated from our derived radii and surface gravity – we refer to these as *spectroscopic masses* as opposed to *evolutionary masses*, derived from stellar evolution tracks.

Fig. 3 shows the positions of our targets in the Hertzsprung-Russsell diagram (HRD), together with the stellar evolution tracks of Heger (1998) for rotating and non-rotating stars with a metallicity Z=0.02; for the relatively massive stars considered here the evolutionary tracks do not depend significantly on the metallicity with those for Z=0.02 and 0.08 being effectively identical. For our targets the means of the luminosities listed in Table 5 were used. Also shown is the HRD transformed into $\log g$– $\log(T_{\rm eff})$ space. The positions of the stars relative to the evolutionary tracks are different in the two HRDs. This has been found previously for massive stars (see Weiss (1994) for an example concerning O-type stars) and implies that two stars can have the same luminosity and effective temperature but different masses and surface gravities. Indeed models that include rotationally induced mixing (for recent discussions see Denissenkov 1994; Talon et al. 1997; Fliegner et al. 1996) confirm that a star's position in the HRD is not uniquely determined by initial stellar mass and metallicity, but that the same position may be reached by stars with differing masses and *rotational velocities*. Furthermore, rotating stars evolve further to the red and to higher luminosities than non-rotating stars – indeed into just that region occupied by the stars considered here. Heger's models illustrate these effects well, but to avoid confusion we have only shown one set of rotating models for an initial equatorial velocity of approximate 200 km s^{-1}.

The fastest rotators are also expected show signs of changes in their surface CNO abundances. Therefore one should expect a correlation between mass-discrepancy (which we define as the difference between the spectroscopic mass and that expected from a star's position in the observational HRD and non-rotating evolution) and chemical composition of our stars.

Table 5. Stellar parameters for a distance-modulus of 11.9

Star	R/R$_{\odot}$	M$_v$	B.C.	M$_{bol}$	log(L/L$_{\odot}$)		M$_{spec}$
					dist.	rad.	
HD 14052	19.4	−5.36	−2.18	−7.54	4.91	4.86	13.6
HD 14053	15.8	−5.01	−2.30	−7.31	4.81	4.76	14.4
HD 14443	21.7	−5.62	−2.18	−7.80	5.01	4.96	17.2
BD +56 502	11.4	−4.32	−2.36	−6.68	4.56	4.52	11.9
BD +56 510	11.8	−4.25	−2.21	−6.46	4.47	4.42	12.6
BD +56 511	14.5	−4.68	−2.13	−6.81	4.61	4.56	9.6
BD +56 576	12.3	−4.22	−2.31	−6.53	4.50	4.47	11.6
BD +56 578	12.1	−4.42	−2.30	−6.72	4.57	4.52	8.4
Oo 2139	4.57	−2.13	−2.20	−4.33	3.62	3.56	7.6
Oo 2196	4.53	−2.07	−2.10	−4.17	3.55	3.50	7.4

Considering first the three bright giants and supergiants – HD 14443 may be nitrogen weak and its mass discrepancy is negligible compared to those for the 'normal' stars HD 14052 and HD 14053, both of which exhibit mild mass discrepancies. This would be consistent with the former being unaffected by rotation, while the latter two objects are mildly nitrogen enriched as the result of faster rotation (note that we only have access to $v \sin i$). The group of fainter giants, BD +56 502, BD +56 576 and BD +56 510, all have small mass discrepancies, implying that rotation is not a major factor in their evolution. However BD +56 510 has the highest $v \sin i$ in our sample (though not necessarily the highest v) and also the highest nitrogen abundance, while the nitrogen abundance of the other two is in good agreement with those of HD 14052 and HD 14053 which we have suggested may actually be nitrogen rich. However the mass constraint may be affected by uncertainties in the gravity estimates; for example, all three stars could have spectroscopic masses as low as $10 M_{\odot}$. The two giants with significant mass discrepancies, BD +56 511 and BD +56 578, are both peculiar with the former being a Be star while the latter may be a spectrum variable (see Sect. 4.3.1).

A striking feature of Fig. 3 is that the variation in stellar mass predicted by rotating models at a given position in the $\log g$–$\log(T_{\rm eff})$ H-R diagram is consistent with our results. For example, HD 14052, HD 14443 and BD +56 511 have masses ranging from 9.6 to 17.2 solar masses and yet they are all have similar atmospheric parameters. However the rotating models have surface [N/C] abundance ratios typically 0.5 dex above their initial values. Such large changes are not observed in our sample which, on the contrary, implies that any abundance variations must be rather small. Hence we conclude that while stellar rotation can explain both the position of our targets within the HRD and the mass discrepancies, we find no significant correlation between the latter and chemical composition.

Obviously a larger sample is really needed to examine these effects. However, boron abundances for these stars would also provide an extremely valuable additonal test of possible rotational mixing as discussed by Fliegner et al. (1996).

5. Discussion and conclusions

In the introduction, we outlined three motivations for this study. Our principal conclusions in these areas are as follows.

- non-LTE model atmosphere techniques would appear to provide reliable atmospheric parameters for early-B-type giants. The estimated microturbulences are relatively large and must be explicitly included in the statistical equilibrium calculations, where they increase theoretical equivalent widths and reduce abundance estimates by typically 0.1 dex but by up to 0.4 dex. The resulting chemical compositions are in reasonable agreement with those deduced for (near) main sequence stars using similar methods.
- There is marginal evidence for variations in the CNO abundances within our sample, with a positive correlation between the N/C abundance ratio and line width; however no correlation is found for the the N/O abundance ratio. Additionally one target, BD +56 578, appears to be a spectrum variable showing on occasions strong nitrogen coupled with weak carbon and oxygen lines. However, it is clear that even using high quality observational data and sophisticated theoretical methods, it remains difficult to identify the relatively small changes in chemical composition predicted by evolutionary models.
- The HRD for our evolved targets appear to be consistent with predictions of evolutionary models including rotation. In particular, such models are consistent with the presence of a significant number of targets in a region where non-rotating models imply that evolution should be very rapid. Additionally rotating models can explain the discrepancies found between spectroscopic masses and the evolutionary masses predicted from non-rotating models. However we find no significant correlation between such mass discrepancies and CNO abundance ratios, nor do the quatitative results match predictions from such models.

Acknowledgements. M.V. acknowledges financial support from the Belgian Federal Scientific Services (DWTC/SSTC). We thank H. Hensberge, E. Griffin and W. Hummel for helpful discussions. This research has made use of the Simbad database, operational at the C.D.S., Strasbourg, France.

References

Anders E., Grevesse N., 1989, Geochim. et Cosmochim. Acta 53, 197
Balona L.A., Shobbrook R.R., 1984, MNRAS 211, 375
Becker S.R., Butler K., 1988, A&A 201, 232
Becker S.R., Butler K., 1989, A&A 209, 244
Becker S.R., Butler K., 1990, A&A 235, 326
Bidelman W.P., 1965, PASP 77, 388
Butler K., Giddings J., 1985, In: Newsletter on Analysis of Astronomical Spectra No. 9, Daresbury Laboratory, Daresbury, England
Code A.D., Davis J., Bless R.C., Hanbury-Brown R., 1976 ApJ 203, 417
Crawford D.L., Glaspey J.W., Perry C.L., 1970, AJ 75, 822
Cunha K., Lambert D.L., 1992, ApJ 399, 586
Cunha K., Lambert D.L., 1994, ApJ 426, 170
Denissenkov P.A., 1994, A&A 287, 113
Dufton P.L., Brown P.J.F., Lennon D.J., Lynas-Gray A.E., 1986, MNRAS 222, 712
Dufton P.L., Brown P.J.F., Fitzsimmons A., Lennon D.J., 1990, A&A 232, 431
Eber F., Butler K., 1988, A&A 202, 153
Fliegner J., Langer N., Venn K.A., 1996, A&A 308, L13
Gies D.R., Lambert D.L., 1992, ApJ 387, 673
Gold M., 1984, Diplomarbeit, Ludwig Maximilians Universität, München
Hambly N.C., Keenan F.P., Brown P.J.F., et al., 1996, ApJ, 466, 1018
Heger A., 1998, Ph.D. Thesis, Technical University of Munich
Herrero A., 1987, A&A 171, 189
Hill G., 1967, ApJS 14, 263
Howarth I.D., Murray J., Mills D., Berry D.S., 1995, Starlink User Notice No. 50.16
Howarth I.D., 1998, Editor of Proceedings of the Second Boulder-Munich Workshop on Properties of Hot luminous stars, PASP Conf. Ser. 131

Husfeld D., 1986, Dissertation Universität München
Johnson H.L., Morgan W.W., 1955, ApJ 122, 429
Kilian J., 1992, A&A 262, 171
Kilian J., 1994, A&A 282, 867
Krzesinski J., Pigulski A., 1997, A&A 325, 987
Kudritzki R.P., 1998, Proceedings of the 7th Canary Island Winter School, in press
Kurucz R.L., 1992, Rev. Mex. Astron. Astrofis. 23, 45
Langer N., 1992, A&A 265, L17
Lehner N., Dufton P.L., Lambert D.L., Ryans R.S.I., Keenan F.P., 2000, MNRAS in press
Lennon D.J., 1983, MNRAS 205, 829
Lennon D.J., Brown P.J.F., Dufton P.L., 1988, A&A 195, 208
Lennon D.J., Dufton P.L., Fitzsimmons A., 1992, A&AS 94, 569
Lennon D.J., Dufton P.L., Mazzali P.A., Pasian F., Marconi G., 1996, A&A, 314, 243
Liu T., Janes K.A., Bania T.M., 1991, AJ 102, 1103
Lyubimkov L.S., 1991, In: Michaud G., Tutukov A., (eds.) Evolution of stars: the photospheric abundance connection. Kluwer, p. 125
Lyubimkov L.S., 1996, Ap&SS 243, 329
Maeder A., 1987, A&A 178, 159
McCarthy J.K., Sandiford B.A., Boyd D., Booth J., 1993, PASP 105, 881
McCarthy J.K., Lennon D.J., Venn K.A., Kudritzki R.P., et al., 1995 ApJ 455, L135
McErlean N.D., Lennon D.J., Dufton P.L., 1998, A&A 329, 613
McErlean N.D., Lennon D.J., Dufton P.L., 1999, A&A 349, 572
Merrill P.W., Burwell C.G., 1950, ApJ 112, 72
Mihalas D., 1972, ApJ 177, 115 A&A 312, 24
Monteverde M.I., Herrero A., Lennon D.J., Kudritzki R.P., 1997, ApJ 474, L107
Nicolet B., 1981, A&A 104, 185
Oosterhoff P.T., 1935, Ann. Sterrenwacht Leiden 17, 1
Paczynski B., 1973, In: Bappu M.K., Sahade J. (eds.) IAU Symp. 49, Evolution aspects of Wolf-Rayet stars. p. 143
Rolleston W.R.J., Brown P.J.F., Dufton P.L., Howarth I.D., 1996, A&A 315, 95
Rolleston W.R.J., Dufton P.L., Fitzsimmons A., Howarth I.D., Irwin M.J., 1993, A&A 277, 10
Rolleston W.R.J., Dufton P.L., McErlean N.D., Venn K.A., 1999, A&A 348, 728
Savage B.D., Sembach K.R., 1996, ARA&A 34, 279
Schild R.E., 1965, ApJ 142, 979
Schild R.E., 1967, ApJ 148, 449
Schönberner D., Harmanec P., 1995, A&A 294, 509
Sigut T.A.A., 1996, ApJ 473, 452
Slettebak A., 1968, ApJ 154, 933
Slettebak A., 1985, ApJS 59, 769
Smartt S.J., Dufton P.L., Rolleston W.R.J., 1996a, A&AS, 116, 483
Smartt S.J., Dufton P.L., Rolleston W.R.J., 1996b, A&A 310, 123
Smartt S.J., Rolleston W.R.J., 1997, ApJ 481, L47
Talon S., Zahn J.-P., Maeder A., Meynet G., 1997, A&A 322, 320
Tapia M., Roth M., Costero R., Navarro S., 1984, Rev. Mex. Astron. Astrofis. 9, 65
Torrejón J.M., Fabregat J., Bernabeu G., Alba S., 1997, A&AS 124, 329
Vrancken M., Butler K., Becker S., 1996, A&A 311, 661
Vrancken M., Hensberge H., David M., Verschueren W., 1997, A&A 320, 878
Waelkens C., Lampens P., Heynderickx D., et al., 1990, A&AS 83, 11
Walborn N.R., 1970, ApJ 161, 149
Walborn N.R., 1976, ApJ 205, 419
Weiss A., 1994, A&A 284, 138
Wildey R.L., 1964, ApJS 8, 439